Obtaining the phase diagram and thermodynamic quantities of bulk systems from the densities of trapped gases

Tin-Lun Ho★ and Qi Zhou★

Experiments that use cold atoms in optical lattices to simulate the behaviour of strongly correlated solid-state systems promise to provide insight into a range of long-standing problems in many-body physics[1-10]. The goal of such 'quantum simulations' is to obtain information about homogeneous systems. Cold-gas experiments, however, are carried out in spatially inhomogeneous confining traps, which leads inevitably to different phases in the sample. This makes it difficult to deduce the properties of homogeneous phases with standard density imaging, which averages over different phases. Moreover, important properties such as superfluid density are inaccessible by standard imaging techniques, and will remain inaccessible even when systems of interest are successfully simulated. Here, we present algorithms for mapping out several properties of homogeneous systems, including superfluid density. Our scheme makes explicit use of the inhomogeneity of the trap, an approach that might turn the source of difficulty into a means of constructing solutions.

To deduce the bulk properties of homogeneous systems from the observed properties of non-uniform systems, local density approximation (LDA) naturally comes to mind. In this approximation, the properties of a non-uniform system at a given point are deduced from their bulk values assuming an effective local chemical potential. To the extent that LDA is valid, determining bulk thermodynamic quantities as functions of chemical potentials amounts to determining their spatial dependencies in confining traps. In present experiments with ultracold atomic gases, column-integrated density (or density for two-dimensional (2D) experiments) is the only local property that can be accessed. No other thermodynamic quantities have been measured because there are no clear ways to access them. Here, we show that by studying changes in density caused by external perturbations, one can access the quantities mentioned above from density data. The deduction of superfluid density is particularly important, as it is a fundamental quantity that has eluded measurement since the discovery of Bose–Einstein condensation.

Our first step is to use the density near the surface of the quantum gas as a thermometer. Within LDA, the density is $n(\mathbf{x}) = n(\mu(\mathbf{x}), T)$, where $n(\mu, T)$ is the density of a homogeneous system with temperature T and chemical potential μ, $\mu(\mathbf{x}) = \mu - V(\mathbf{x})$; $V(\mathbf{x}) = 1/2\, M \sum_{i=x,y,z} \omega_i^2 x_i^2$ is a harmonic trapping potential with frequencies ω_i and M is the mass of the atom. Near the surface, the density is sufficiently low that one can carry out a fugacity expansion to obtain

$$n(\mathbf{x}) = \alpha e^{(\mu - V(\mathbf{x}))/k_B T}/\lambda^3 \qquad (1)$$

where $\lambda = h/\sqrt{2\pi M k_B T}$ is the thermal wavelength and k_B is the Boltzman constant. For a p-component quantum gas in a single trap, we have $\alpha = p$. If the quantum gas is in the lowest band of a cubic lattice with hopping integral t and lattice spacing d, then $\alpha = p(\lambda/d)^3[I_0(2t/k_B T)]^3$, where $I_0(x)$ is the Bessel function of the first kind (see the Methods section). The corresponding column density $\tilde{n}(x,y) = \int n(x,y,z)dz$ (with $\mathbf{r} = (x,y)$) is

$$\tilde{n}(x,y) = \alpha \left(\frac{k_B T}{\hbar \omega_z} \right) \frac{e^{(\mu - V(\mathbf{r}))/k_B T}}{\lambda^2} \qquad (2)$$

Equation (2) has been widely used to determine μ and T of quantum gases in single traps but not yet for gases in optical lattices, as the density at the surface in such cases is very low. The lack of accurate thermometry in optical lattices has been the bottleneck for extracting information from present experiments. For example, it has prevented mapping out the phase diagram of the Bose–Hubbard model at finite temperature despite many years of studies. It has also given rise to concern about heating effects in current optical lattice experiments[11–14]. To make use of the asymptotic forms in equations (1) and (2), we need imaging resolutions comparable to a few lattice spacings (typically a few micrometres). Recently, the density of a 3D quantum gas has been imaged using a focused electron beam with extremely high resolution (0.15 μm; ref. 15). Furthermore, advances in optical imaging techniques have also enabled resolutions from a few lattice spacings[10] to even one lattice spacing (M. Greiner, reported in APS March Meeting, 2009). These developments show that the capability to determine μ and T accurately using density measurements at the surface is now in place.

Before proceeding, we would like to point out that LDA has been verified in a large number of boson and fermion experiments[9,10] and numerical calculations[16,17]. For the rest of our discussions, we shall assume that LDA is valid. One might also worry about poor signal-to-noise ratios for the density near the surface. However, by averaging over a surface layer of thickness of one or two lattice spacings, one can obtain a considerable enhancement of the signal-to-noise ratio even at the surface[10,17].

With μ and T determined from the surface density, one readily obtains the equation of state $n(\nu, T)$ by identifying it with $n(\mathbf{x})$, where x is given by $V(\mathbf{x}) = \mu - \nu$. In present experiments on 3D systems, only column density $\tilde{n}(x,y) = \int n(x,y,z)dz$ is measured. To deduce $n(\mathbf{x})$ from $\tilde{n}(x,y)$, one can use the inverse Abel transform in the case of cylindrically symmetric samples[9], or a method developed by E. Mueller (private communication). The latter method first constructs the pressure P from $\tilde{n}(x,y)$,

Department of Physics, The Ohio State University, Columbus, Ohio 43210, USA. *e-mail: ho@mps.ohio-state.edu; qzhou@mps.ohio-state.edu.
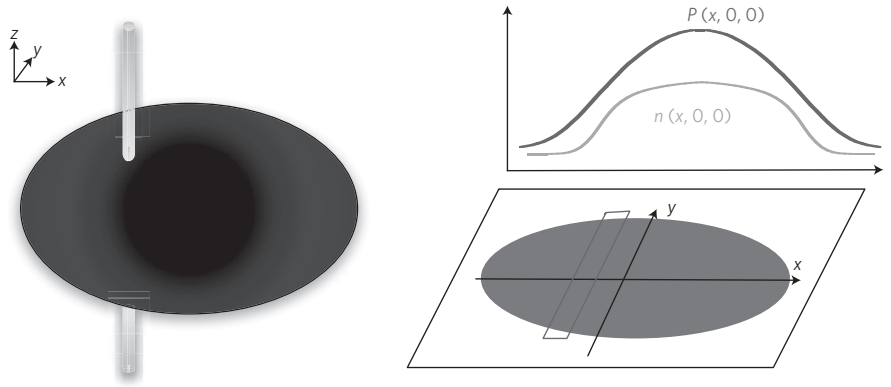
Figure 1 | An illustration of the method to construct pressure from column density. The 3D quantum gas is represented by a ellipse. The rod represents the column density collected in the experiment. By integrating the column density along the y direction, as shown in the rectangle, one obtains $\tilde{n}(x)$, and hence $P(x, 0, 0)$ from equation (3). The density $n(x, 0, 0)$ can be obtained by differentiating $P(x, 0, 0)$ as in equation (4).
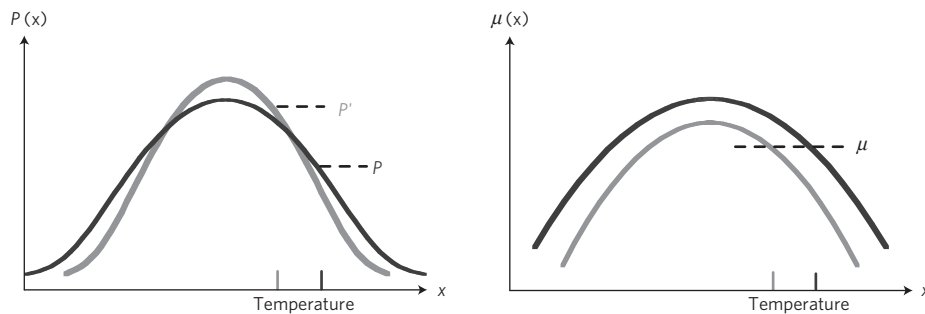

Figure 2 | An illustration of the scheme for determining entropy density s(x). The pressure curve $P(x, 0, 0)$ and effective chemical potential $\mu(x)$ of the initial state with temperature T are shown as black lines. The corresponding quantities of the final state are shown as grey lines. The final equilibrium state is generated from the initial state by changing the trap frequency from ω to ω' adiabatically. To find $s(x)$, we find the position x' related to x, with an identical effective local chemical potential, by equating $\mu(x, 0, 0) = \mu'(x', 0, 0)$. The pressures at x and x' are denoted as P and P' in the figure. $s(x)$ is given by equation (5).

and then $n(\mathbf{x})$ from the pressure. It works as follows: from the Gibbs–Duham equation,

$$dP = n\,d\mu + s\,dT \qquad (3)$$

we have $P = \int n\,d\mu$ if T is constant. By integrating the column density along y, $\tilde{n}(x) = \int \tilde{n}(x, y)\,dy = \int n(\mu - 1/2M\sum_{i=x,y,z}\omega_i^2 x_i^2, T)\,dy\,dz$, and noting that $dy\,dz = -(2\pi/M\omega_y\omega_z)d\mu$ for given x, we have

$$P(x, 0, 0) = \frac{M\omega_y\omega_z}{2\pi}\tilde{n}(x)$$

Again applying the Gibbs–Duham relation, we then get the 3D density (see Fig. 1)

$$n(x, 0, 0) = \left(\frac{\partial P}{\partial \mu(x)}\right)_T = -\frac{1}{2\pi x}\frac{\omega_y\omega_z}{\omega_x^2}\frac{d\tilde{n}(x)}{dx} \qquad (4)$$

As singularities of thermodynamic potentials show up in the equation of state, boundaries between different phases can be identified in the density profile. Recall that first-order and continuous phase transitions correspond to discontinuities in the first- and higher-order derivatives of P. Equation (3) implies that n and s are discontinuous across a first-order phase boundary, whereas the slope of $dn/d\mu$ and ds/dT are discontinuous for higher-order phase boundaries. The discontinuity in n has been used in a recent experiment to determine the first-order phase boundary in spin-polarized fermions near unitarity[9].

As $dn(x, 0, 0)/dx \propto dn(\mu(x, 0, 0), T)/d\mu$, a higher-order phase boundary will show up as a discontinuity of the slope of the density. The presence of such a discontinuity has also been seen in Monte Carlo studies[17].

We now turn to entropy density $s(\mathbf{x})$, which is useful for identifying phases. For example, for a spin-1/2 fermion Hubbard model, if $s(\mathbf{x})$ is far below $k_B\ln 2$ per site in a Mott phase, this is strong evidence for spin ordering. To obtain $s = (dP/dT)_\mu$, we need to generate two slightly different configurations of $P(\mathbf{x})$ with different T and calculate their difference at the same μ. To do this, we change the trap frequency ω_x adiabatically to a slightly different value ω_x' ($\omega_x' = \omega_x + \delta\omega_x, \delta\omega_x \ll \omega_x$). Both μ and T will then change to a slightly different value, for example, to μ' and T' (ref. 11). One can then measure the column density of the final state and construct its pressure function $P(x, 0, 0)$. The entropy density of the initial state along the x axis is

$$s(x, 0, 0) = \frac{P'(x', T') - P(x, T)}{T' - T} \qquad (5)$$

where x and x' are related to each other as follows (see Fig. 2):

$$\mu(x) \equiv \mu - \frac{1}{2}M\omega_x^2 x^2 = \mu' - \frac{1}{2}M\omega_x'^2 x'^2 \equiv \mu'(x')$$

We next consider superfluid density n_s. It is a quantity particularly important for 2D superfluids[18–20], as the famous Kosterlitz–Thouless transition is reflected in a universal jump in superfluid density. Without a precise determination of n_s, interpretation of

experimental results, be they based on quantum Monte Carlo simulations or on features of an interference pattern, will be indirect. Here, we propose a scheme to measure the inhomogeneous superfluid density in the trap. For a superfluid, we have[21,22]

$$\mathrm{d}P = n\,\mathrm{d}\mu_{\mathrm{o}} + s\,\mathrm{d}T - Mn_{\mathrm{s}}\mathbf{w}\cdot\mathrm{d}\mathbf{w} \qquad (6)$$

where n_{s} is the superfluid number density and $\mathbf{w} = \mathbf{v}_{\mathrm{s}} - \mathbf{v}_{\mathrm{n}}$; $\mathbf{v}_{\mathrm{s}}$ and $\mathbf{v}_{\mathrm{n}}$ are the superfluid and normal fluid velocity, respectively. The term μ_{o} corresponds to the chemical potential in the $\mathbf{v}_{\mathrm{n}} = 0$ frame. A direct consequence of equation (6) is that

$$\left(\frac{\partial n}{\partial w^2}\right)_{\mu_{\mathrm{o}},T} = -\frac{M}{2}\left(\frac{\partial n_{\mathrm{s}}}{\partial\mu_{\mathrm{o}}}\right)_{w^2,T} \qquad (7)$$

For a potential rotating along $\hat{z}$ with frequency $\Omega, \mathbf{v}_{\mathrm{n}} = \Omega\hat{z}\times\mathbf{x}$. If Ω is below the frequency for vortex generation, $\mathbf{v}_{\mathrm{s}} = 0$ and $w^2 = \Omega^2 r^2$. As $\mathbf{w}$ varies in space, we cannot apply the method developed for $s(\mathbf{r})$. Instead, one can use the following procedure: let $n^{(i)}(\mathbf{x})$ be the density of a stationary system (with temperature T and chemical potential $\mu^{(i)}$) in a cylindrical trap with transverse frequency $\omega_{\perp}^{(i)}$ and longitudinal frequency ω_z. Within LDA, we have, $n^{(i)}(\mathbf{x}) = n(\mu^{(i)}(\mathbf{x}); T; \mathbf{w} = \mathbf{0})$, where

$$\mu^{(i)}(\mathbf{x}) = \mu^{(i)} - \frac{1}{2}M\omega_{\perp}^{(i)2}r^2 - \frac{1}{2}M\omega_z^2 z^2$$

We then rotate this system with frequency Ω along $\hat{z}$, and adjust $\omega_{\perp}^{(i)}$ to $\omega_{\perp}^{(f)}$, so that the temperature remains T. The chemical potential then becomes $\mu^{(f)}$, and the density of this final state is $n^{(f)}(\mathbf{x}) = n(\mu^{(f)}(\mathbf{x}), T, \mathbf{w})$, where

$$\mu^{(f)}(\mathbf{x}) = \mu^{(f)} - \frac{1}{2}M(\omega_{\perp}^{(f)2} - \Omega^2)r^2 - \frac{1}{2}M\omega_z^2 z^2$$

For small w^2, we have

$$n(\mu^{(f)}(\mathbf{x}), T, \mathbf{w}) = n(\mu^{(f)}(\mathbf{x}), T, \mathbf{0}) + \left(\frac{\partial n}{\partial w^2}\right)_{\mu^{(f)}, w=0} w^2$$

We then write $n(\mu^{(f)}(\mathbf{x}), T, 0) = n(\mu^{(i)}(\mathbf{x}^*), T, 0) = n^{(i)}(\mathbf{x}^*)$, where $\mathbf{x}^* = (x^*, y^*, z^*)$ is the point that satisfies $\mu^{(f)}(\mathbf{x}) = n^{(i)}(\mathbf{x}^*)$. Specifically, we can choose $z^* \equiv z, 1/2\,M\omega_{\perp}^{(i)2}y^{*2} \equiv 1/2M(\omega_{\perp}^{(f)2} - \Omega^2)y^2$, and $\mu^{(i)}(x^*, 0, 0) \equiv \mu^{(f)}(x, 0, 0)$. Using equation (7), we have

$$\frac{n^{(f)}(\mathbf{x}) - n^{(i)}(\mathbf{x}^*)}{M\Omega^2(x^2 + y^2)/2} = -\left(\frac{\partial n_{\mathrm{s}}}{\partial\mu^{(f)}}\right)_{w=0} \qquad (8)$$

where $n_{\mathrm{s}}(x, y, z) = n_{\mathrm{s}}(\mu^{(f)}(\mathbf{x}), T, \mathbf{0})$. Integrating equation (8) over z and y, and noting that $\mathrm{d}y\mathrm{d}z = -2\pi/M\omega_z\sqrt{\omega_{\perp}^{(i)2} - \Omega^2}\mathrm{d}\mu^{(f)}$ when x is constant, we have

$$n_{\mathrm{s}}(x, 0, 0) = \frac{\omega_z\sqrt{\omega_{\perp}^{(f)2} - \Omega^2}}{\pi\Omega^2}\int\mathrm{d}y\frac{\tilde{n}^{(i)}(x^*, y^*) - \tilde{n}^{(f)}(x, y)}{(x^2 + y^2)} \qquad (9)$$

Equation (9) gives n_{s} in terms of the column densities of the initial and final state. The above formula continues to hold for non-axisymmetric traps (with $\omega_{\perp}^{(f)} \to \omega_y^{(f)}$). (See also Supplementary Material for the expression for the 2D case, and an alternative scheme for obtaining $n_{\mathrm{s}}(\mathbf{x})$.)

Our method can also be applied to obtain other important thermodynamic properties such as the staggered magnetization and the contact density of a strongly interacting fermion gas. For the latter, see Supplementary Materials. In quantum simulations of the fermion Hubbard model using two-component fermions in optical lattices[23,24], the measurement of the staggered magnetization will be crucial for identifying the antiferromagnet. Consider an antiferromagnet in a cubic lattice with a staggered magnetic field, $\mathbf{h}(\mathbf{x}) = \hat{z}e^{i\pi(n_x + n_y + n_z)}\bar{h}$, where $\mathbf{x} = (n_x, n_y, n_z)d$ are the lattice sites, n_i are integers, d is the lattice spacing and $\bar{h}$ is the magnitude of the staggered field. The Hamiltonian for a homogeneous system is $H = H_{\mathrm{H}} - \sum_{\mathbf{x}}\tilde{m}_{\mathrm{op}}(\mathbf{x})\bar{h}$, where H_{H} is the Hubbard Hamiltonian, $\tilde{m}_{\mathrm{op}}(\mathbf{x}) = \hat{z}e^{i\pi(n_x + n_y + n_z)}m_z(\mathbf{x})$ is the staggered-magnetization operator and $\mathbf{m}(\mathbf{x})$ is the spin operator at $\mathbf{x}$. Antiferromagnetism corresponds to $\tilde{m} = \langle\tilde{m}_{\mathrm{op}}\rangle \neq 0$ as $\bar{h} \to 0$. It is straightforward to show that

$$\mathrm{d}P = n\,\mathrm{d}\mu + s\,\mathrm{d}T + \tilde{m}\,\mathrm{d}\bar{h}$$

The staggered field $\mathbf{h}(\mathbf{x})$ has been produced recently[25]. To reduce spontaneous emission and hence heating, one can use a low-intensity laser and hence a weak field $\bar{h}$. Note that even a weak field can produce large changes in density in the spatial region close to the antiferromagnetic phase boundary, where bulk spin susceptibility $\mathrm{d}\tilde{m}/\mathrm{d}\bar{h}$ diverges. So, measuring the responses to $\bar{h}$ can locate the phase boundary.

As $\tilde{m} = (\partial P/\partial\bar{h})_{\mu,T}$, we need to generate two configurations of P with different $\bar{h}$ while fixing μ and T. We begin with an initial state with $\bar{h} = 0$, and determine its μ, T and pressure $P(x, 0, 0)$ as discussed above. We then turn on a weak $\bar{h}$ adiabatically. At the same time, we adjust ω to a new value ω', so that the temperature of the final state remains fixed at T, and the chemical potential is changed to $\bar{\mu}'$. We then construct the pressure $P'(x, 0, 0)$ of the final state. By noting that for any point $(x', 0, 0)$ in the final state, one finds a corresponding point $(x, 0, 0)$ in the initial state such that their effective chemical potentials are identical, that is, $\mu(x, 0, 0) \equiv \mu - (1/2)M\omega^2 x^2 = \mu' - (1/2)M\omega'^2 x'^2 \equiv \mu'(x', 0, 0)$. We then have

$$\tilde{m}(x, 0, 0) = \frac{P'(\mu'(x', 0, 0), T, \bar{h}) - P(\mu(x, 0, 0), T, 0)}{\bar{h}}$$

The success in deducing the properties of bulk homogeneous systems hinges on two key factors. The first is the ability to determine the density, temperature and chemical potential of the trapped system with high accuracy. The second is to come up with algorithms to deduce the bulk properties of interest from the density data of non-uniform systems. A combination of precision measurements and specifically designed algorithms, aiming to uncover the properties of bulk systems both qualitative and quantitative will be crucial in realizing the full power of quantum simulation.

Methods

Equation (1) is derived as follows: near the surface, the gas is in the low-fugacity limit. The number density can then be obtained by fugacity expansion. To the lowest order in fugacity, the number of particles per site of a (homogeneous p-component) quantum gas in a cubic lattice is

$$\frac{N}{N_{\mathrm{site}}} = \frac{p}{N_{\mathrm{site}}}e^{\mu\beta}\sum_{\mathbf{k}\in BZ}e^{-\varepsilon_{\mathbf{k}}\beta}$$

where the k-sum is over the first Brillouin zone, $\varepsilon_{\mathbf{k}} = -2t\sum_{i=x,y,z}\cos k_i d$, d is the lattice constant and t is the tunnelling integral. In the continuum limit, the above expression becomes

$$\frac{N}{N_{\mathrm{site}}} = pe^{\mu\beta}d^3\prod_{i=x,y,z}\left(\int_{-\pi}^{\pi}\frac{\mathrm{d}k_i}{2\pi}e^{2t\beta\cos k_i d}\right) = pe^{\mu\beta}I_0(2t\beta)^3$$

where $I_0(x)$ is the Bessel function of the first kind. The number of particles per unit volume is then

$$n = \frac{N}{d^3 N_{\mathrm{site}}} = p\left(\frac{\lambda I_0(2t\beta)}{d}\right)^3\frac{e^{\mu\beta}}{\lambda^3}$$

where $\lambda = h/\sqrt{2\pi Mk_{\mathrm{B}}T}$ is the thermal wavelength.

References

1. Greiner, M., Mandel, O., Esslinger, T., Hänsch, T. W. & Bloch, I. Quantum phase transition from a superfluid to a Mott insulator in a gas of ultracold atoms. *Nature* **415,** 39–44 (2002).
2. Xu, K. *et al.* Observation of strong quantum depletion in a gaseous Bose–Einstein condensate. *Phys. Rev. Lett.* **96,** 180405 (2006).
3. Chin, J. K. *et al.* Evidence for superfluidity of ultracold fermions in an optical lattice. *Nature* **443,** 961–964 (2006).
4. Günter, K., Stöferle, T., Moritz, H., Köhl, M. & Esslinger, T. Bose–Fermi mixtures in a three-dimensional optical lattice. *Phys. Rev. Lett.* **96,** 180402 (2006).
5. Ospelkaus, S. *et al.* Localization of bosonic atoms by fermionic impurities in a three-dimensional optical lattice. *Phys. Rev. Lett.* **96,** 180403 (2006).
6. Spielman, I. B., Phillips, W. D. & Porto, J. V. Condensate fraction in a 2D Bose gas measured across the Mott-insulator transition. *Phys. Rev. Lett.* **100,** 120402 (2008).
7. Schneider, U. *et al.* Metallic and insulating phases of repulsively interacting fermions in a 3D optical lattice. *Science.* **322,** 1520–1525 (2008).
8. Jördens, R., Strohmaier, N., Günter, K., Moritz, H. & Esslinger, T. A Mott insulator of fermionic atoms in an optical lattice. *Nature* **455,** 204–207 (2008).
9. Shin, Y., Schunck, C.H., Schirotzek, A. & Ketterle, W. Phase diagram of a two-component Fermi gas with resonant interactions. *Nature* **451,** 689–693 (2007).
10. Gemelke, N., Zhang, X., Hung, C.-L. & Chin, C. *In situ* observation of incompressible Mott-insulating domains of ultracold atomic gases. *Nature* **460,** 995–998 (2007).
11. Ho, T. L & Zhou, Q. Intrinsic heating and cooling in adiabatic processes for bosons in optical lattices. *Phys. Rev. Lett.* **99,** 120404 (2007).
12. Cramer, M. *et al.* Do mixtures of bosonic and fermionic atoms adiabatically heat up in optical lattices? *Phys. Rev. Lett.* **100,** 140409 (2008).
13. Pollet, L., Kollath, C., Houcke, K. V. & Troyer, M. Temperature changes when adiabatically ramping up an optical lattice. *New. J. Phys.* **10,** 065001 (2008).
14. Yoshimura, S., Konabe, S. & Nikuni, T. Adiabatic cooling and heating of cold bosons in three-dimensional optical lattices and the superfluid–normal phase transition. *Phys. Rev. A.* **78,** 015602 (2008).
15. Gericke, T., Würtz, P., Reitz, D., Langen, T. & Ott, H. High-resolution scanning electron microscopy of an ultracold quantum gas. *Nature Phys.* **4,** 949–953 (2008).
16. Trotzky, S. *et al.* Suppression of the critical temperature for superfluidity near the Mott transition: Validating a quantum simulator. Preprint at <http://arxiv.org/abs/0905.4882> (2009).
17. Zhou, Q., Kato, Y., Kawashima, N. & Trivedi, N. Direct mapping of finite temperature phase diagram of strongly correlated quantum models. *Phys. Rev. Lett.* **103,** 085701 (2009).
18. Hadzibabic, Z., Krüger, P., Cheneau, M., Battelier, B. & Dalibard, J. B. Berezinskii–Kosterlitz–Thouless crossover in a trapped atomic gas. *Nature* **441,** 1118–1121 (2006).
19. Krüger, P., Hadzibabic, Z. & Dalibard, J. Critical point of an interacting two-dimensional atomic Bose gas. *Phys. Rev. Lett.* **99,** 240402 (2008).
20. Cladé, P., Ryu, C., Ramanathan, A., Helmerson, K. & Phillips, W. D. Observation of a 2D Bose-gas: From thermal to quasi-condensate to superfluid. *Phys. Rev. Lett.* **100,** 120402 (2008).
21. Khalatnikov, I. M. *An Introduction to the Theory of Superfludity* (W. A. Benjamin, 1965).
22. Ho, T. L. & Shenoy, V. B. The hydrodynamic equations of superfluid mixtures in magnetic traps. *J. Low Temperature Phys.* **111,** 937–952 (1998).
23. Greiner, M. & Fölling, S. Optical lattices. *Nature* **453,** 736–738 (2008).
24. Cho, A. The mad dash to make light crystals. *Science* **320,** 312–313 (2008).
25. Trotzky, S. *et al.* Time-resolved observation and control of superexchange interactions with ultracold atoms in optical lattices. *Phys. Rev. Lett.* **101,** 155303 (2008).

Author contributions

All authors contributed extensively to the work presented in this letter.

Additional information

The authors declare no competing financial interests. Supplementary information accompanies this paper on www.nature.com/naturephysics. Reprints and permissions information is available online at http://npg.nature.com/reprintsandpermissions. Correspondence and requests for materials should be addressed to T.-L.H. or Q.Z.